Applied Microbiology and Biotechnology (2019) 103:8087–8103
https://doi.org/10.1007/s00253-019-10047-2

APPLIED GENETICS AND MOLECULAR BIOTECHNOLOGY

A cytochrome P450 monooxygenase gene required for biosynthesis of the trichothecene toxin harzianum A in *Trichoderma*

Rosa E. Cardoza[1] · Susan P. McCormick[2] · Laura Lindo[1] · Hye-Seon Kim[2] · Elías R. Olivera[3] · David R. Nelson[4] · Robert H. Proctor[2] · Santiago Gutiérrez[1]

Received: 13 May 2019 / Revised: 15 July 2019 / Accepted: 23 July 2019 / Published online: 5 August 2019

Abstract

Trichothecenes are sesquiterpene toxins produced by diverse fungi, including some species of *Trichoderma* that are potential plant disease biocontrol agents. *Trichoderma arundinaceum* produces the trichothecene harzianum A (HA), which consists of the core trichothecene structure (12,13-epoxytrichothec-9-ene, EPT) with a linear polyketide-derived substituent (octa-2,4,6-trienedioyl) esterified to an oxygen at carbon atom 4. The genes required for biosynthesis of EPT and the eight-carbon polyketide precursor of the octa-2,4,6-trienedioyl substituent, as well as for esterification of the substituent to EPT have been described. However, genes required for conversion of the polyketide (octa-2,4,6-trienoic acid) to octa-2,4,6-trienedioyl-CoA, the immediate precursor of the substituent, have not been described. Here, we identified 91 cytochrome P450 monooxygenase genes in the genome sequence of *T. arundinaceum*, and provided evidence from gene deletion, complementation, cross-culture feeding, and chemical analyses that one of them (*tri23*) is required for conversion of octa-2,4,6-trienoic acid to octa-2,4,6-trienedioyl-CoA. The gene was detected in other HA-producing *Trichoderma* species, but not in species of other fungal genera that produce trichothecenes with an octa-2,4,6-trienoic acid-derived substituent. These findings indicate that *tri23* is a trichothecene biosynthetic gene unique to *Trichoderma* species, which in turn suggests that modification of octa-2,4,6-trienoic acid during trichothecene biosynthesis has evolved independently in some fungi.

Keywords *Trichoderma* trichothecenes · Harzianum A · Cytochrome P450 monooxygenase · Genome sequencing · Transcriptomics · Secondary metabolites

Introduction

Trichothecenes are sesquiterpenoid toxins produced by some species in diverse fungal genera (Pitt et al. 2017; Proctor et al. 2018), including plant and insect pathogens (Kikuchi et al. 2004), and some saprotrophs, such as *Trichoderma arundinaceum* and *T. brevicompactum*. Collectively, trichothecene-producing fungi have been reported to produce over 150 structurally distinct trichothecene analogs, all of which share the same core structure, 12,13-epoxytrichothec-9-ene (EPT), but differ in patterns and types of oxygenations and acylation at one or more positions of EPT (McCormick et al. 2011; Proctor et al. 2018). The genus *Trichoderma* includes multiple species used as biological control agents of important fungal phytopathogens (Harman et al. 2004). In addition, some *Trichoderma* strains have been shown to increase plant growth and to stimulate plant defenses against biotic and abiotic damage (Shoresh et al. 2010; Hermosa et al. 2012; Rubio et al. 2017); many species have been

Electronic supplementary material The online version of this article (https://doi.org/10.1007/s00253-019-10047-2) contains supplementary material, which is available to authorized users.

✉ Robert H. Proctor
robert.proctor@ars.usda.gov

✉ Santiago Gutiérrez
s.gutierrez@unileon.es

[1] Area of Microbiology, University of León, Campus de Ponferrada, Ponferrada, Spain

[2] National Center for Agricultural Utilization Research, United States Department of Agriculture, Peoria, IL, USA

[3] Area of Biochemistry and Molecular Biology, University of León, León, Spain

[4] Dept. of Microbiology, Immunology and Biochemistry, University of Tennessee, Memphis, TN, USA

described as plant-beneficial microorganisms. However, trichothecene production in *Trichoderma* species has raised concerns about whether these species are pathogenic on plants, because trichothecene production in some *Fusarium* species contributes to their pathogenicity on plants. Furthermore, the *Trichoderma* trichothecene trichodermin is toxic to plants (Malmierca et al. 2012). In contrast, the *T. arundinaceum* or *T. albolutescens* trichothecenes harzianum A (HA) and 16-hydroxy-trichodermin are much less phytotoxic, and the species that produce them (*T. arundinaceum* or *T. albolutescens*) have the ability to protect plants against fungal and viral pathogens (Malmierca et al. 2012; Ryu et al. 2017). Thus, trichothecene production in some *Trichoderma* species has potential to contribute to biological control of plant disease despite the phytotoxicity of some analogs.

Harzianum A (HA) consists of EPT with an eight-carbon, polyketide-derived acyl group (octa-2,4,6-trienedioyl) esterified to an oxygen at carbon atom 4 (C4) (Fig. 1). Molecular genetic and biochemical analyses of *T. arundinaceum* have identified most HA biosynthetic genes (*tri*) and, thereby, the corresponding proteins (TRI). These analyses indicate that the HA biosynthetic pathway consists of three distinct phases: (1) an early phase that leads to the formation of a trichodermol (4-hydroxy-EPT); (2) another early phase that leads to the formation of octa-2,4,6-trienedioyl-CoA; and (3) a late phase in which octa-2,4,6-trienedioyl replaces the 4-*O*-acetyl group of trichodermin, which results in formation of HA (Fig. 1) (Cardoza et al. 2011; Lindo et al. 2018, 2019a, b; Proctor et al. 2018).

The proposed trichodermol phase (early phase 1) of the HA pathway begins when a terpene synthase, TRI5, catalyzes transformation of the primary metabolite farnesyl diphosphate (FPP) to the terpene trichodiene. A cytochrome P450 monooxygenase (CYP), TRI4, then catalyzes three oxygenations of trichodiene that result in formation of EPT. Finally, another CYP, TRI22, catalyzes hydroxylation of EPT at carbon atom 4 (C4) to form trichodermol (Cardoza et al. 2011). The proposed octa-2,4,6-trienedioyl-CoA phase of the HA pathway begins when a polyketide synthase, TRI17, catalyzes formation of the linear eight-carbon polyketide, octa-2,4,6-trienoic acid (Proctor et al. 2018). This molecule then undergoes multiple modifications that result in formation of a second carboxyl group at C8 and, thereby formation of octa-2,4,6-trienedioic acid. The latter molecule is then ligated to CoA to form octa-2,4,6-trienedioyl-CoA. This conversion of octa-2,4,6-trienoic acid to octa-2,4,6-trienedioyl-CoA is predicted to require hydroxylase, alcohol dehydrogenase, aldehyde dehydrogenase, and acyl-CoA synthase activities (Proctor et al. 2018), but genes encoding enzymes with these activities specific for trichothecene biosynthesis have not been identified.

In the late phase of the HA biosynthetic pathway, an acyltransferase, TRI3, catalyzes 4-*O*-acetylation of trichodermol to form 4-acetyl EPT (trichodermin). Then, another acyltransferase, TRI18, catalyzes a transacylation reaction that results in replacement of the 4-acetyl with octa-2,4,6-trienedioyl to form HA (Lindo et al. 2019a).

In *T. arundinaceum*, the *tri* genes that have been identified are located at one of three loci. The first locus consists of a cluster of seven *tri* genes, including *tri3*, *tri4*, and *tri22*. This cluster also includes: *tri12*, which encodes an efflux pump; *tri6* and *tri10*, which encode regulatory proteins; and *tri14*, which encodes a protein of unknown function (Cardoza et al. 2011; Proctor et al. 2018). The second *tri* locus includes only one known *tri* gene, *tri5* (Alexander et al. 1999; Cardoza et al. 2011), and the third locus includes *tri17* and *tri18* with a CYP gene located between them (Proctor et al. 2018). In fungi, genes in a secondary metabolite biosynthetic gene cluster typically exhibit similar patterns of expression. Furthermore, expression of the clustered genes is often regulated by a transcription factor encoded by a gene in the cluster. This is the case for the *T. arundinaceum tri* cluster. That is, the regulatory proteins TRI6 and TRI10 are required for induction of expression of the structural genes in the *tri* cluster as well as for expression of the known *tri* genes at other loci (i.e., *tri5*, *tri17*, and *tri18*) (Lindo et al. 2018, 2019a).

The objective of the current study was to identify genes involved in conversion of the polyketide octa-2,4,6-trienoic acid to octa-2,4,6-trienedioyl-CoA. Through a series of experiments, we identified a CYP gene, *tri23*, that is required for synthesis of HA but not for synthesis of trichodermol. These and other characteristics of *tri23* are consistent with the hypothesis that it is involved in conversion of octa-2,4,6-trienoic acid to octa-2,4,6-trienedioic acid.

Material and methods

Strains used and culture conditions

Trichoderma arundinaceum IBT 40837 (Ta37) (IBT Culture Collection of Fungi, Lyngby, Denmark) was used as wild-type strain for deletion of *tri23* gene. All *Trichoderma* strains used in the present work were maintained on a PDA medium (PDB (Difco) with 2% agar) and grown at 28 °C for 7 days in the dark. Similar conditions were used for sporulation, but using PPG medium (2% mashed potatoes, 2% glucose, 2% agar) and incubated at 28 °C in the dark.

For RNA isolation, *Trichoderma* strains were grown as previously described (Lindo et al. 2018). Briefly, first, strains were inoculated in 50 mL of CM broth (0.5% malt extract, 0.5% yeast extract, 0.5% glucose), in 250 mL flasks, and incubated for 24 h at 28 °C and 250 rpm. Ten mL of this preinoculum were transferred to 250 mL flasks containing

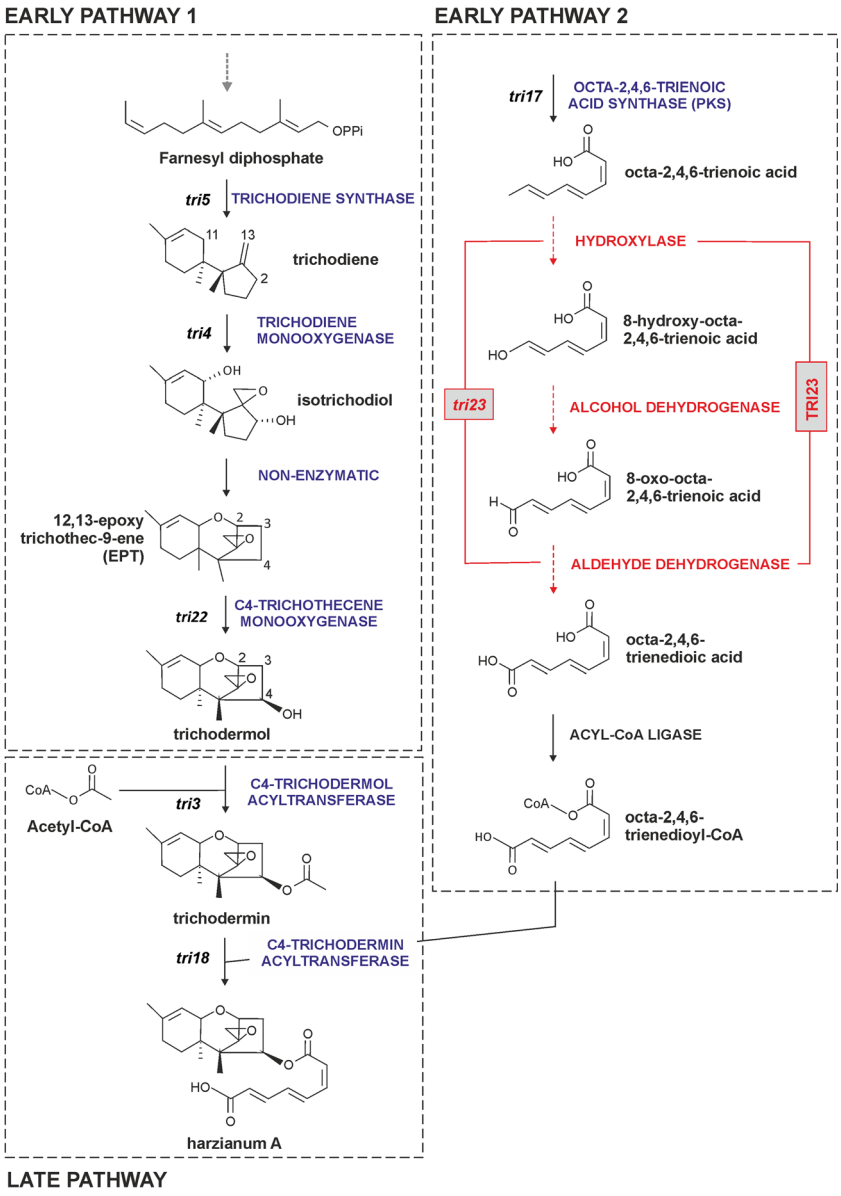

Fig. 1 Proposed harzianum A biosynthetic pathway in *Trichoderma arundinaceum* divided into three phases: early pathway 1 (=early phase 1), early pathway 2 (=early phase 2), and late pathway (=late phase). Genes are indicated in bold and black lowercase letters in italics, and enzymes are indicated by bold and blue uppercase letters. The potential activities of TRI23, as deduced in the current study, are indicated by red text in Early Pathway 2

50 mL PDB medium and grown for 48 h also at 28 °C and 250 rpm. Mycelia were recovered by filtration through sterile Miracloth (Calbiochem), freeze-drying, and used for RNA extraction.

Botrytis cinerea B05.10, which was isolated from a vineyard (Quidde et al. 1998), was the pathogen assayed in the antifungal assays. *B. cinerea* B05.10 was sporulated in V8 medium (Oxoid Ltd.) and incubated for 7 days in a growth chamber at 21 °C and a photoperiod of 16 h light/8 h dark.

Construction of plasmid pΔtri23 for *T. arundinaceum tri23* deletion

A 1082 bp fragment of the Ta37 *tri23*-5′ region (*tri23* promoter region) was amplified using Taq DNA polymerase (Eurx) and tri23-5F /tri23-5R primers (Table S1), containing *Bam*HI and *Eco*RV restriction sites, respectively, and genomic DNA of Ta37 as template. This fragment was phosphorylated with T4-DNA polynucleotide kinase (Fermentas), purified using the "PCR and band purification" kit (GE Healthcare), and cloned into pBluescript KS+ (Stratagene) previously digested with *Bam*HI-*Eco*RV. The resulting plasmid, pBtri23-5′ (4082 bp), was digested with *Eco*RV and *Xho*I and ligated to the 1062 bp fragment, corresponding to the Ta37 *tri23*-3′ region (*tri23* terminator region) that was PCR amplified from Ta37 genomic DNA, using the oligonucleotides tri23-3F/tri23-3R (Table S1) and Taq DNA polymerase (Eurx). This fragment was digested, after the PCR amplification, with *Eco*RV-*Xho*I endonucleases, and gel purified as indicated above, prior to the ligation. As a result, plasmid pBtri23-5′3′(5144 bp) was obtained, digested with *Eco*RV, treated with alkaline phosphatase-CIAP (Fermentas) and finally ligated to a

2702 bp fragment, containing the hygromycin B resistance cassette from pAN7-1 (Punt et al. 1987) that had been digested with *Ecl*136II-*Hin*dIII and filled with Klenow (Thermo Scientific) (Fig. S1a). The resulting plasmid (pΔtri23) was linearized with *Kpn*I prior to transformation of *T. arundinaceum* protoplasts.

Construction of plasmids pTCtri23-b1 and pPtri23-b1

Plasmid pTCtri23-b1 A fragment of 1747 bp, corresponding to the complete Ta-*tri23* ORF lacking the initial ATG was amplified using the Q5 polymerase (NE Biolabs), primers tri23-5Fb/tri23-3Rb (Table S1), and genomic DNA of Ta37 as template. The resulting fragment was phosphorylated using T4-polynucleotide kinase (Fermentas) and ligated to the plasmid pTACBH2S** previously digested with *Nco*I and treated with Klenow fragment (Fermentas) and alkaline phosphatase, giving rise to the plasmid pTCtri23b (7087 bp). Plasmid pTACBH2S** was prepared from plasmid pTACBH2 (Cardoza et al. 2015) by digestion with *Sal*I, filing-in with the Klenow fragment and autoligation, and the same process repeated for *Sac*II endonuclease, resulting in the inactivation of the *Sal*I and *Sac*II sites.

Plasmid pTCtri23b was digested with *Bgl*II, treated with Klenow, dephosphorylated with alkaline phosphatase-CIAP, and ligated to the phleomycin resistance cassette (1595 bp), which was isolated from plasmid pJL43b1 (Cardoza et al. 2006) by digestion with *Ecl*136II-*Hin*dIII, gel extracted and filling-in with Klenow fragment, to give rise to the final plasmid pTCtri23-b1 (Fig. S1b). This plasmid was linearized with *Nar*I to transform protoplasts of mutant strain Δtri23.74.

Plasmid pPtri23-b1 A 3758 bp fragment, containing the entire genomic Ta37-*tri23* ORF, and including its 5′-promoter and 3′-terminator regions, was amplified using the Q5 polymerase, the oligonucleotides tri23-promF/tri23-termR (Table S1), and Ta37 genomic DNA as template. The fragment was phosphorylated with T4-DNA polynucleotide kinase and ligated to pJL43b1 (Cardoza et al. 2006), previously digested with Ecl136II and treated with CIAP, giving rise to plasmid pPtri23-b1 (Fig. S1c). This plasmid was linearized with *Kpn*I and used to transform protoplasts of the mutant strain Δtri23.74.

Fungal transformation

Transformations of wild-type and mutant (Δtri23.74) strains of *T. arundinaceum* were carried out according to previously described procedures (Cardoza et al., 2006; Proctor et al. 1999). Selection of *tri23* deleted transformants was carried out in regeneration medium (Malmierca et al. 2012) supplemented with 150 μg/mL hygromycin, while *tri23*-complemented transformants, isolated from protoplasts of Δtri23.74, were selected in Czapek medium with 1 M sorbitol and supplemented with 100 μg/mL phleomycin. The selected transformants were analyzed by Terra PCR (Takara Bio) using the primer pairs described below.

Metabolite analysis

HA was quantitated by HPLC analysis of ethyl acetate extracts of 48-h liquid PDB cultures as previously described (Cardoza et al. 2011; Lee et al. 2005). Under these conditions, HA eluted at approximately 22 min, and was quantitated by comparison of the peak area versus a standard curve.

Gas chromatography-mass spectrometry (GC-MS) analysis was used to assess production of trichothecene analogs other than HA. *T. arundinaceum* strains were grown for 7 d in 20 mL of YEPD (50 g yeast extract, 1 g peptone, 1 g dextrose per 1 L water), and broths were extracted with 8 mL of ethyl acetate. Extracts were dried under a nitrogen stream, and the residue was resuspended in 1 mL of ethyl acetate. GC-MS analysis was performed on a 6890 Gas Chromatograph and a 5973 mass detector (Agilent) as previously described (Lindo et al. 2018). The column used was 30 m × .25 mm i.d., 0.25 μm, (5%-phenyl)-methylpolysiloxane (HP-5MS, Agilent, Wilmington DE).

For ergosterol analysis, mycelia obtained by filtration of 48-h PDB cultures were extracted with *n*-heptane, and the ergosterol levels in the extracts were determined as previously described (Lindo et al. 2019a). All samples were assayed in duplicate, and production values of HA and ergosterol were analyzed by the IBM SPSS Statistics 24 software, using analysis of variance with a post-hoc Tukey test.

Antifungal assays

Antibiograms against *Botrytis cinerea* B05.10 were carried out as previously described (Malmierca et al. 2015).

Genome sequencing and analysis

For sequencing the genome of Δtri23.74 mutant, DNA was extracted from mycelium grown for 6 d on a CM solid medium using ZR fungal/bacterial DNA MiniPrep Kit (Zymo Research Co.). The DNA sequencing library was prepared using the Nextera XT DNA library Preparation Kit (Illumina Inc.), according to manufacturer's instructions. Genome sequence data for Δtri23.74 mutant strain was obtained using a MiSeq Illumina platform (Illumina Inc.) as described previously (Lindo et al. 2019a).

Sequence data were processed using CLC Genomics Workbench (Qiagen). Mapping of the genome sequence reads to reference sequences was done using the Read Mapping function in the CLC Genomics Workbench. Genomic sequence reads for the wild-type strain *T. arundinaceum* IBT 40837 were generated in a previous study (GenBank accession number PXOA00000000) (Proctor et al. 2018; Lindo et al. 2018) and used for comparative analysis in the current work.

Phylogenetic analysis

To construct the P450 phylogenetic trees, the 91 *T. arundinaceum* cytochrome P450 monooxygenases (CYP), were added to a previously analyzed collection of 184 fungal P450s previously analyzed (Nelson 2018). These protein sequences were first aligned using CLUSTAL (Sievers et al. 2011), and evolutionary analyses were computed with the same software. The phylogenetic tree was inferred by using the neighbor-joining method (Saitou and Nei 1987) for the alignment containing both, the sequences from the Nelson fungal P450 database (Nelson 1999, 2018) and the P450s from Ta37. Visualization and customization were accomplished using Figtree 1.4.4 software (tree.bio.ed.ac.uk/software/figtree). Furthermore, these proteins were also aligned using MAFFT v.7 (Katoh et al. 2002; Nakamura et al. 2018), and evolutionary analyses were computed with the IQ-Tree software 1.6.10 (Nguyen et al. 2014). The phylogenetic tree was inferred by using the maximum likelihood method. Bootstrap analysis was performed using 1000 pseudoreplicates. Visualization and customization were accomplished as indicated above.

In order to identify the conserved signature motifs in the selected CYP, sequences were aligned with the program MEGA program (Kumar et al. 2016) using the clustal-Ω algorithm (Sievers et al. 2011; Sievers and Higgins 2014). Consensus Logos of the alignments were generated by WebLogo 3 software (Crooks et al. 2004).

Assignment of *T. arundinaceum* CYPs to the different existing CYP families and CYP Clans was carried out according to the International P450 Nomenclature Committee Databases, on the basis of the highest homologies observed in the BlastP comparisons against the fungal P450 database (http://drnelson.uthsc.edu/cytochromeP450.html) (Nelson 1999).

Based on standard nomenclature for the Cytochrome P450 monooxygenase superfamily, and even when some families have exceptions to the following criteria, members of the same family originally had > 40% amino acid sequence identity, and subfamily members > 55% identity. The families sharing a common phylogenetic origin, assumed by bootstrap values > 70%, are grouped forming a Clan (Hillis and Bull 1993).

RNA-seq and real-time PCR analyses

For analysis of expression of CYP genes in the Ta37 genome, we used a previously generated RNA-seq dataset derived from mRNAs of wild-type strain Ta37 and a *tri6* deletion mutant (Δtri6.66) that were grown for 24 h in PDB medium (GenBank accession number SRP156794) (Lindo et al. 2018). The cDNA libraries were sequenced, trimmed and mapped to the previously reported genome sequence of strain Ta37 (Lindo et al. 2018).

For qPCR analysis primers for *T. arundinaceum tri4*, *tri22*, *tri17*, *tri18*, *tri23*, and the actin gene (as a housekeeping gene) were as described previously (Lindo et al. 2019b). The amplification efficiencies of the primers was between 92.5 and 105%. RNAs were extracted, from mycelia grown as indicated above, using Trizol Reagent (Life Technologies), treated with RNase free-DNase and purified through Zymo-Spin™ columns (Zymo Research Co.). cDNAs were synthesized using the iScriptTM cDNA synthesis kit (BIO-RAD), following the manufacturer's instructions, and quantitated using a Nanodrop ND-1000 (ThermoFisher) prior to be used for qPCR analysis. qPCR reactions were carried out using the Step One system (Applied Biosystems) and the Express SYBR green qPCR super-Mix Universal (Invitrogen) as previously described (Lindo et al. 2019b; Malmierca et al. 2012). The resulting data were analyzed with REST© 2009 software (Pfaffl et al. 2002) to determine expression levels for each gene/condition normalized to amplification efficiencies of each primer pair and to expression of the actin gene. Each measurement was done in triplicate.

Results

Identification of *tri23*

We identified 95 putative cytochrome P450 monooxygenase (CYP) genes in the annotated genome sequence of *T. arundinaceum* (Lindo et al. 2018; Proctor et al. 2018). Examination of the deduced amino acid sequences of the genes indicated that four lacked conserved domains typical of CYPs. As a result, the four genes were excluded from subsequent analyses. Thus, the genome sequence of *T. arundinaceum* was predicted to have 91 CYP genes, which were assigned to 63 CYP families (Table S2). Nineteen of these families have not been previously reported in *Trichoderma* species (Chadha et al. 2018).

We surmised that genes required for conversion of octa-2,4,6-trienoic acid to octa-2,4,6-trienedioic acid would be regulated by TRI6 and exhibit patterns of expression similar those of known *tri* genes. Following this rationale, we examined the pattern of expression of the 91 putative CYP genes in *T. arundinaceum* using previous generated RNA-seq data

from a *tri6* mutant of the fungus (Lindo et al. 2018). Seventeen of the genes exhibited patterns of expression similar to those of known *tri* genes; i.e., they were down-regulated in the *tri6* deletion mutant (Fig. 2a). Two of the genes were the previously described *tri4* and *tri22*. Among the other 15 CYP genes, one was located between *tri17* and *tri18*. This gene was previously designated as TARUN_5178 in the annotated genome sequence of *T. arundinaceum* Ta37 (Proctor et al. 2018), and here we further designated it as *tri23* (Fig. 2a, b).

In silico analysis of *tri23*

Sanger sequence analysis of cDNA clones indicated that the *tri23* ORF was 1746 bp long and is interrupted by three introns of 79, 55, and 82 bp (Fig. S2). The predicted TRI23 protein has 510 amino acids, a molecular mass of 58 kDa, and a theoretical pI of 8.3. TRI23 was predicted to have one transmembrane domain at amino acids 6–27 according to the TMHMM, Phobius, TMPred, and NHTM software (Fig. S3) (Hofmann and Stoffel 1993; Käll et al. 2004; Krogh et al. 2001). Transmembrane domains at amino acids 301–320 and 450–472 were also predicted by some, but not all, of the software packages. No signal peptides were detected in TRI23 by SignalP-4.1 prediction software (Petersen et al. 2011).

Use of the *tri23* coding region as a query sequence in BLASTx analysis of the Nelson fungal P450 database (http://drnelson.uthsc.edu /cytochromeP450.html) (Nelson 1999) revealed that TRI23 has high levels of similarity to multiple CYPs. The highest similarities were to *Cryphonectria* CYP5336B1 (e-140) and CYP5336B2 (e-121), *Trichophyton rubrum* CYP5335A2 (e-105), *Microsporum canis* CYP5336A4 (e-103), and *Leptosphaeria maculans* CYP5336E1 (e-102).

CYP domains in Ta-TRI23 CYPs are an important superfamily of enzymes involved in multiple processes such as xenobiotics degradation, primary and secondary metabolism, and fungal-

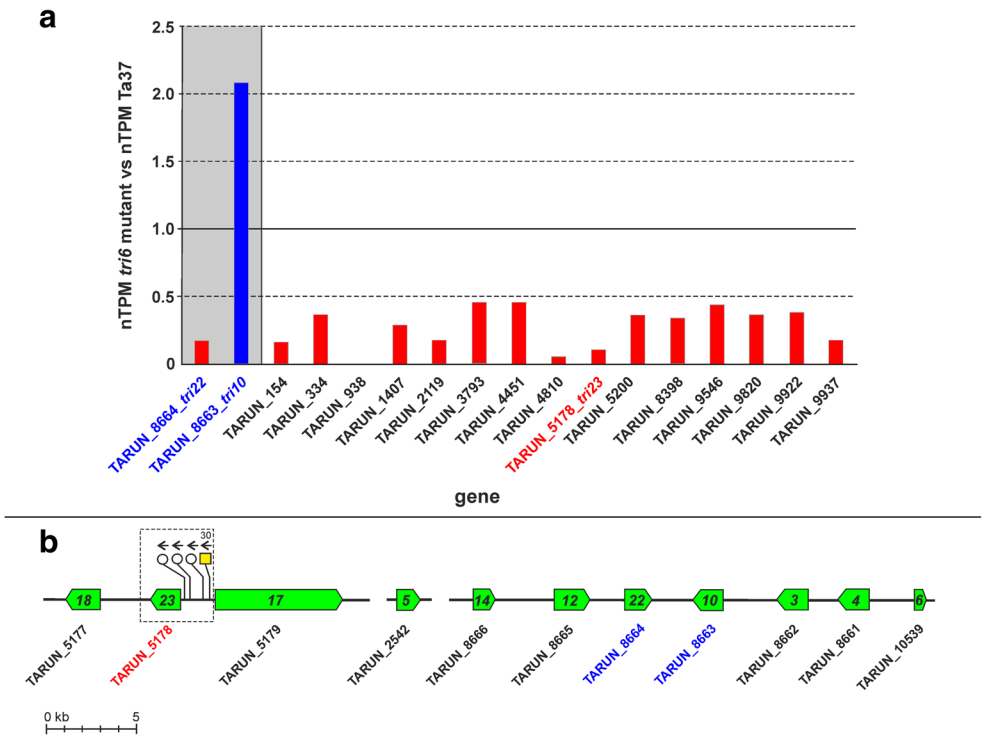

Fig. 2 **a** Relative transcription level of 15 selected *T. arundinaceum* cytochrome P450 monooxygenase (CYP) genes in a *tri6* deleted mutant versus the level of expression in the wild-type strain deduced from a RNA-seq analysis (Lindo et al. 2018). The nTPM values are the transcripts per million reads (TPM) for each gene normalized against the TPM of the actin gene on each sample (*tri6* mutant or Ta37). Relative transcription levels of *tri22* (TARUN_8664_*tri22*) and *tri10* (TARUN_8663_*tri10*) genes (gray rectangle) were included for comparative purposes (Lindo et al. 2018). Gene model TARUN_5178 (red text) corresponds to *tri23*. **b** Organization of trichothecene biosynthetic loci in *T. arundinaceum*. Green arrows indicate predicted position and direction of transcription of the genes. Numbers within arrows indicate *tri* gene designation (e.g., *23* indicates *tri23*). Numbers below arrows are locus tag numbers assigned to each gene by in silico characterization of the genome sequence (Lindo et al. 2018). The open circles and yellow box indicate positions of putative TRI6-binding sequences in the promoter region of - *T. arundinaceum tri23* gene. The open circles indicate the binding sequence TNAGGCC described by Hohn et al. (1999), and the yellow square indicates the binding sequence GTGA-(6-50)-GTGA identified by Nasmith et al. (2011). The number above the yellow square indicates the distance in nucleotides between the two tandem copies of GTGA in this putative TRI6-binding motif. Arrows above the symbols indicate the strand in which the binding sequence motifs were located. Only binding sequences oriented in the direction of *tri23* transcription are shown

plant interactions. Despite the wide variation in amino acid sequences of these enzymes, there are several motifs that are conserved throughout the superfamily (Lamb et al. 2002). The AGXDTT motif contributes to oxygen-binding and activation (Chen et al. 2014), and the EXXR and PERW motifs are important for locking the heme into position and to assure stabilization of the core structure. The two latter domains are followed by the heme binding region FXXGXXXCXG, which is the most conserved motif, that includes the axial Cys ligand (bold-underlined C) (Chen et al. 2014; Poulos and Johnson 2005; Werck-Reichhart and Feyereisen 2000). Further analysis indicated that these CYP-specific domains are also present in two other known *T. arundinaceum* trichothecene biosynthetic CYP, TRI4, and TRI22, (Cardoza et al. 2011, 2015; Lindo et al. 2018; Proctor et al. 2018). These conserved domains were also detected in other *T. arundinaceum* CYPs in the Clan CYP53, but the degree of amino acid sequence conservation was lower (Fig. 3b-d). Phylogenetic analysis using the neighbor-joining (NJ) or maximum likelihood (ML) methods revealed that 42 of the 91 *T. arundinaceum* CYPs, including TRI4, TRI22, and TRI23, belong to the P450 monooxygenase clan CYP53. This suggests a common evolutionary origin for these 42 enzymes (Fig. 3a, Fig. S4a, b). Furthermore, even when the NJ and ML trees inferred from the CYP alignment were similar, not all CYPs resolved in Clan CYP53 in the NJ tree were resolved as a monophyletic clade in the ML tree (Fig. S4a, b). Nevertheless, the three trichothecene biosynthetic CYPs from *T. arundinaceum* were resolved within a monophyletic clade that included all (NJ tree) or most (ML tree) members of Clan CYP53 described by Nelson (2018).

Distribution of *tri23* In BLAST analysis in which *tri23* was used as the query, orthologs of *tri23* were not detected in other fungi, including those reported to produce trichothecenes and/or have other trichothecene biosynthetic genes; e.g., *Beauveria bassiana*, *Cordyceps confragosa*, *Fusarium graminearum*, *F. longipes*, *F. sporotrichioides*, *Microcyclospora tardicrescens*, *Myrothecium roridum*, *Spicellum ovalisporum*, *S. roseum*, *Stachybotrys chartarum*, *S. chlorohalonata*, and *Trichothecium roseum.* In order to determine if *tri23* occurs in other trichothecene-producing *Trichoderma* species, we used *tri23* as a query sequence in BLASTn analysis of recently generated genome sequences of *T. albolutescens*, *T. brevicompactum*, *T. protrudens*, *T. turrialbense*, and *Hypocrea rodmanii*. Orthologs of *tri23* were detected in *T. protrudens* and *T. turrialbense*, which produce HA, but not in *T. albolutescens* and *T. brevicompactum*, which produce trichodermin. *Hypocrea rodmanii* produces trichodermin rather than HA even though a preliminary analysis indicated that the fungus has a *tri23* ortholog. However, a more detailed analysis indicated that the *H. rodmanii tri23* has a 285-bp deletion at its 3′ end, which likely renders the gene nonfunctional and is consistent with the production of trichodermin rather than HA.

Deletion of *tri23*

Transformation of wild-type *T. arundinaceum* strain Ta37 with the *tri23* deletion plasmid, pΔtri23, and subsequent selection on hygromycin amended media yielded 92 transformants. Analysis of these transformants by Terra PCR (Takara Bio.) using oligonucleotides tri23-1F / tri23-1R (Table S1) identified three transformants, Δtri23.37, Δtri23.39, and Δtri23.74, in which *tri23* could not be detected (Fig. S5a). Subsequent PCR analysis of the three transformants yielded the 1450 bp and 1225 bp amplicons expected to result from replacement of the *tri23* coding region with the hygromycin resistance cassette (Fig. 4a; Fig. S5b, c). As a result, the three transformants were selected for further analyses.

Genome sequence analysis indicated that the *tri23* coding region was absent in transformant Δtri23.74, and that only one copy of the hygromycin resistance gene, *hph*, had integrated into the genome at the *tri23* locus (Fig. 4b). In addition, no sequences corresponding to the *tri23*-deletion construct were detected outside the *tri23* locus (Fig. 4c). Thus, both PCR and genome sequence analyses indicated that strain Δtri23.74 is a *tri23* deletion mutant with only one copy of the hygromycin resistance cassette integrated into the genome.

Metabolite production by *tri23* mutants

HPLC analysis of 48 h PDB cultures indicated that deletion mutants Δtri23.39 and Δtri23.74 did not produce detectable levels of HA. In contrast, the wild-type progenitor strain produced 201 μg HA per mL of culture (Fig. 5a). Furthermore, GC-MS analyses revealed that the *tri23* mutants produced higher levels of trichodermol and aspinolides compared to the wild type (Fig. 5b, Fig. S6). The latter result was similar to those previously observed for HA-nonproducing strains of *T. arundinaceum* generated by inactivation of *tri17*, *tri3*, and *tri18*.

tri23 mutants exhibited a slight, but not statistically significant, decrease in ergosterol production, which is in contrast with results observed in most previously described *T. arundinaceum tri* mutants (Lindo et al. 2019a; Proctor et al. 2018; Laura Lindo and Rosa E. Cardoza, unpublished data) (Table S3).

Complementation of tri23 mutant

The *tri23* mutant, strain Δtri23.74, was complemented using two approaches. In the first approach, *tri23* expression was driven by the *tss1* promoter (plasmid pTCtri23-b1), which results in high levels of constitutive expression. In the second

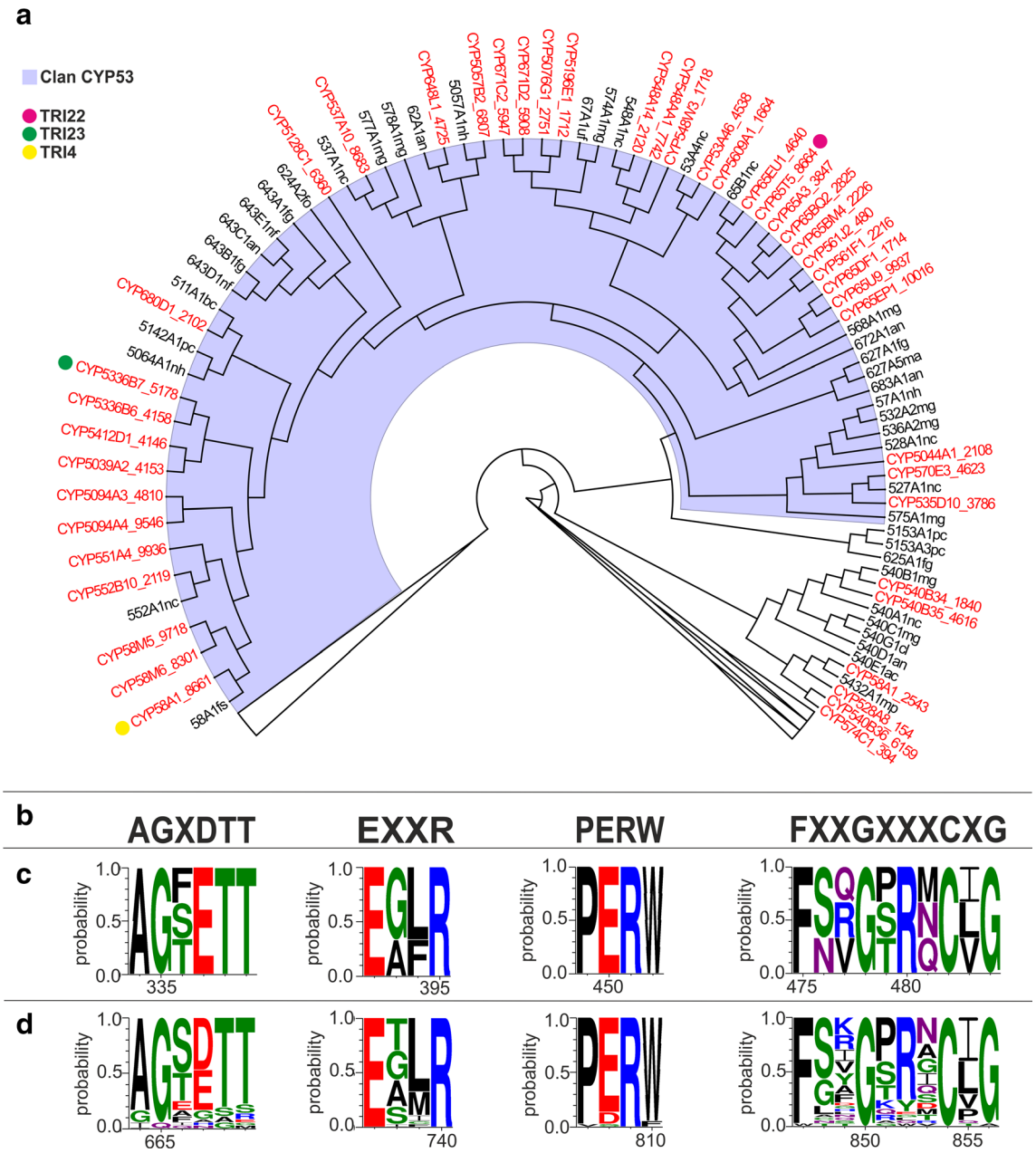

Fig. 3 **a** Clan CYP53 region of a phylogenetic tree inferred by neighbor-joining analysis of the fungal CYPs described by Nelson (2018; black text) and *T. arundinaceum* CYPs (red text). The *T. arundinaceum* CYPs involved in trichothecene biosynthesis (i.e., TRI4, TRI22 and TRI23) are indicated by colored dots. **b** Amino acid sequences of four conserved motifs that occur in fungal CYPs. **c** Consensus sequences for the conserved motifs in the *T. arundinaceum* CYPs involved in trichothecene biosynthesis: TRI4 (=CYP58A1; gene model TARUN_8661), TRI22 (=CYP65T5; gene model TARUN_8664), and TRI23 (=CYP5336B7; gene model TARUN_5178). **d** Consensus sequences for the four conserved motifs in all 42 *T. arundinaceum* CYPs that are members of Clan CYP53, including TRI4, TRI22, and TRI23. Consensus sequence was determined using WebLogo (http://weblogo.threeplusone.com/create.cgi) (Schneider and Stephens 1990; Crooks et al. 2004). The four conserved motifs correspond to amino acids 311-316, 369-372, 425-428, and 444-453 in the *T. arundinaceum* TRI23 protein. The uncompressed tree showing all clans is presented in Fig. S4

approach, *tri23* expression was driven by the native *tri23* promoter, which resulted in wild-type expression.

On average, 20 transformants were obtained per regeneration plate following transformation of *tri23* mutant Δtri23.74 with complementation plasmid pPtri23-b1 (Fig. S1). In PCR analysis with oligonucleotides tri23_5 / tri23_3 (Table S1), a subset of 32 transformants yielded the 1463-bp amplicon expected from integration of the complementation plasmid into the genome (Fig. S7a). Transformants Δtri23-PP2, 8, 12, and 19 were arbitrarily selected for further analysis. In PDB medium, two of these transformants (Δtri23-PP2 and Δtri23-PP8)

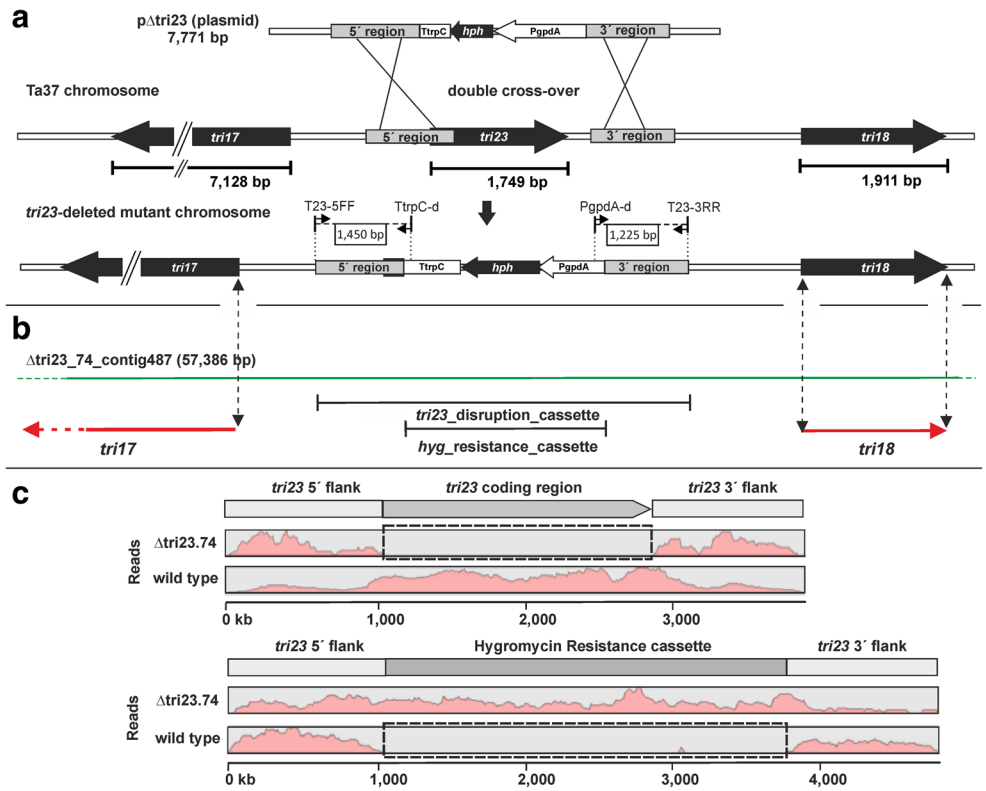

Fig. 4 **a** Strategy used to delete the *tri23* gene of *T. arundinaceum* by double cross-over using pΔtri23 plasmid, in the lower scheme of this panel there are shown the two fragments of 1450 bp and 1225 bp amplified by PCR and sequenced to confirm the *tri23*-deleted mutants. **b** Analysis using Sequencher Software (Gene Codes Co.) of the *tri17-tri23-tri18* genomic region in the Δtri23.74 mutant. **c** Mapping of genome sequence reads to the wild-type *tri23* region (lower panels), and the *tri23* deletion construct (upper panels). In each experiment, the Read Mapping function in CLC Genomics Workbench was used to map the genome sequence reads from the wild-type progenitor strain, Ta37 (wild type), or the *tri23* deletion mutant Δtri23.74, to the reference sequences. The pink areas indicate the number of reads for a given region of the reference sequence. The higher the pink area indicated a greater coverage of that region. The absence of pink in a given region of the reference sequence indicates that no reads cover that region (dotted black rectangles). No other plasmid sequences were detected in the genome of the selected mutant

produced HA at 91–181 μg/mL. These values are 45–90% of the levels produced by the wild-type progenitor strain (201 μg/mL) (Fig. 6c, e).

Furthermore, an average of 10 transformants was obtained from each regeneration plate following transformation with complementation plasmid pTCtri23-b1 (Fig. S1). In PCR analysis with oligonucleotides tri23_5/tri23_3, a subset of 20 transformants yielded the expected 1463-bp amplicon. Four of these transformants (Δtri23-TC1, 5, 9, and 16) were arbitrarily selected for further analyses (Fig. S7b). In PDB cultures, transformants Δtri23-TC1 and Δtri23-TC5 produced 134–244 μg HA/mL. This corresponded to 66–121% of the HA levels produced by the wild-type progenitor strain (Fig. 6d, e).

GC-MS analysis of complemented *tri23* mutant strains Δtri23-PP8 and Δtri23-TC5 indicated that trichodermol production was reduced relative to the mutant Δtri23.74 from which they were derived, and were similar levels to those produced by the wild-type progenitor strain (Fig. 7). These data indicate that cultures of *tri23* mutants accumulated trichodermol as result of a block in HA biosynthesis.

Cross-culture of *tri23* and *tri17* mutants

In *T. arundinaceum*, *tri3*, *tri18*, and *tri17* are required for formation and esterification of the octa-2,4,6-trienedioyl substituent of HA (Proctor et al. 2018; Lindo et al. 2019a). Deletion of any one of these genes blocks HA production and results in accumulation of trichodermol, the same trichothecene phenotype as the *tri23* mutants. This phenotype combined with the fact that TRI23 is predicted to be a CYP is consistent with the hypothesis that TRI23 catalyzes hydroxylation of octa-2,4,6-trienoic acid, the predicted polyketide product of TRI17 and precursor of octa-2,4,6-trienedioic acid. Thus, both TRI17 and TRI23 should be required for synthesis of octa-2,4,6-trienedioic acid. If *tri23* mutants are blocked in formation of octa-2,4,6-trienedioic acid, a precursor of this metabolite may accumulate in the mutants and could be released into media in which the mutants are grown. If this is the case, another strain of *T. arundinaceum* blocked at an earlier step in octa-2,4,6-trienedioic acid formation (e.g., formation of the polyketide octa-2,4,6-

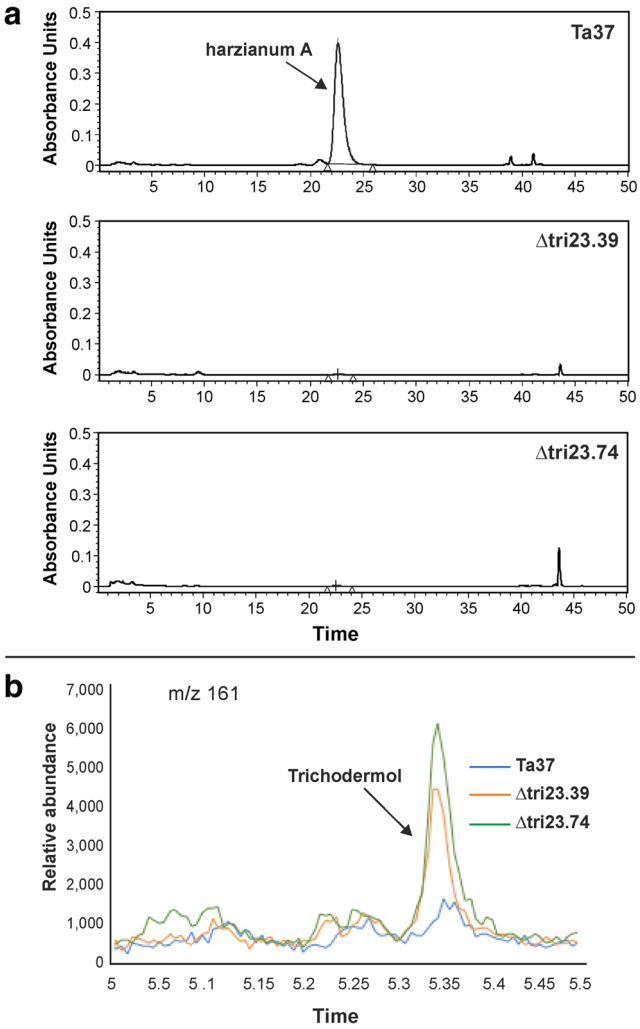

Fig. 5 **a** HPLC chromatograms showing levels of harzianum A produced by wild-type *T. arundinaceum* (Ta37) and two *tri23* deletion mutants, Δtri23.39 and Δtri23.74, grown for 48 h in PDB medium. **b** Gas chromatography-mass spectrometry analysis of extracts of 7-day-old YEPD cultures of the wild-type *T. arundinaceum* strain Ta37 and the *tri23* deletion mutant strains Δtri23.39 and Δtri23.74. The chromatograms show metabolites with *m/z* (mass-to-charge) 161, which is characteristic of trichodermol

trienoic acid) might be able to modify the precursor and thereby use it to synthesize HA (Fig. 8). To test whether this is possible, *tri23* mutant strain Δtri23.74 was grown in PDB medium. After 48 h, the culture broth was harvested by filtration, extracted twice with ethyl acetate, and evaporated to dryness in a rotary evaporator. The solid residue was resuspended in 50 mL PDB and heat sterilized. The resulting amended PDB medium was then inoculated with mycelia of *tri17* mutant strain Δtri17.139, which had been grown for 24 h in an unamended PDB medium and harvested by filtration. This culture was grown for an additional 48 h, after which the broth was analyzed by HPLC for HA (Fig. S8). HA was not detected in the PDB culture broth of the *tri17* or *tri23* mutants, when either mutant was grown alone (Fig. 8a, c). However, HA was produced by the *tri17* mutant when it was grown in PDB amended with extract from the *tri23* mutant (Fig. 8b). In addition, no HA was produced when the *tri23* mutant was grown in PDB medium amended with extract from the *tri17* mutant (Fig. 8d). These data indicate that TRI17 and TRI23 are required for synthesis of the octa-2,4,6-trienedioyl substituent of HA, and that TRI23 acts after TRI17 in the HA biosynthetic pathway (Fig. 1).

Expression of *tri23* in complemented *tri23* mutants

Expression of *tri23* was strongly upregulated in all *tri23*-complemented transformants analyzed compared to the wild-type progenitor strain. Furthermore, the complemented transformants in which *tri23* expression was driven by the *tss1* gene promoter (plasmid pTCtri23-b1) exhibited higher levels of expression than when expression was controlled by the endogenous promoter (plasmid pPtri23-b1). Thus, in comparison with expression of the actin gene, *tri23* expression was 500 fold higher (*p(H1)* = 0.0) in Δtri23-TC5 transformant, while this value for Δtri23-PP8 reached only 1.4-fold (*p(H1)* = 0.0) (Fig. 9a). However, there was not a clear correlation between *tri23* expression and levels of HA produced. Thus, in transformant Δtri23-TC5, *tri23* expression was strongly upregulated, compared with the wild type, but HA production was only 23% higher. Furthermore, no increases in HA production were observed in complemented mutants in which *tri23* expression was driven by the native promoter (Fig. 6e).

Effect of *tri23*-deletion and -complementation on the transcription level of other *tri* genes

We used qPCR to examine effects of *tri23* deletion and complementation on expression of other *tri* genes that varied in genomic location and in the phase of the trichothecene biosynthesis in which they function (i.e., early phase 1, early phase 2 or late phase; Fig. 1). *tri17* and *tri18* are located adjacent to and on either side of *tri23*, and they function in the early phase 2 and late phase, respectively. In 48 h cultures, these two genes exhibited increased expression in the *tri23* mutant relative to the wild type, and even higher levels of expression following complementation of the *tri23* mutant (Fig. 9b). *tri4* and *tri22* are located distal to *tri23*, in the *tri* cluster, and they function during early phase 1 of trichothecene biosynthesis. *tri4* and *tri22* exhibited patterns of expression that were similar to those of *tri17* and *tri18*; that is, expression was higher in the *tri23* mutant than in the wild type, and expression was higher in the complemented *tri23* mutant than in the mutant (Fig. 9b).

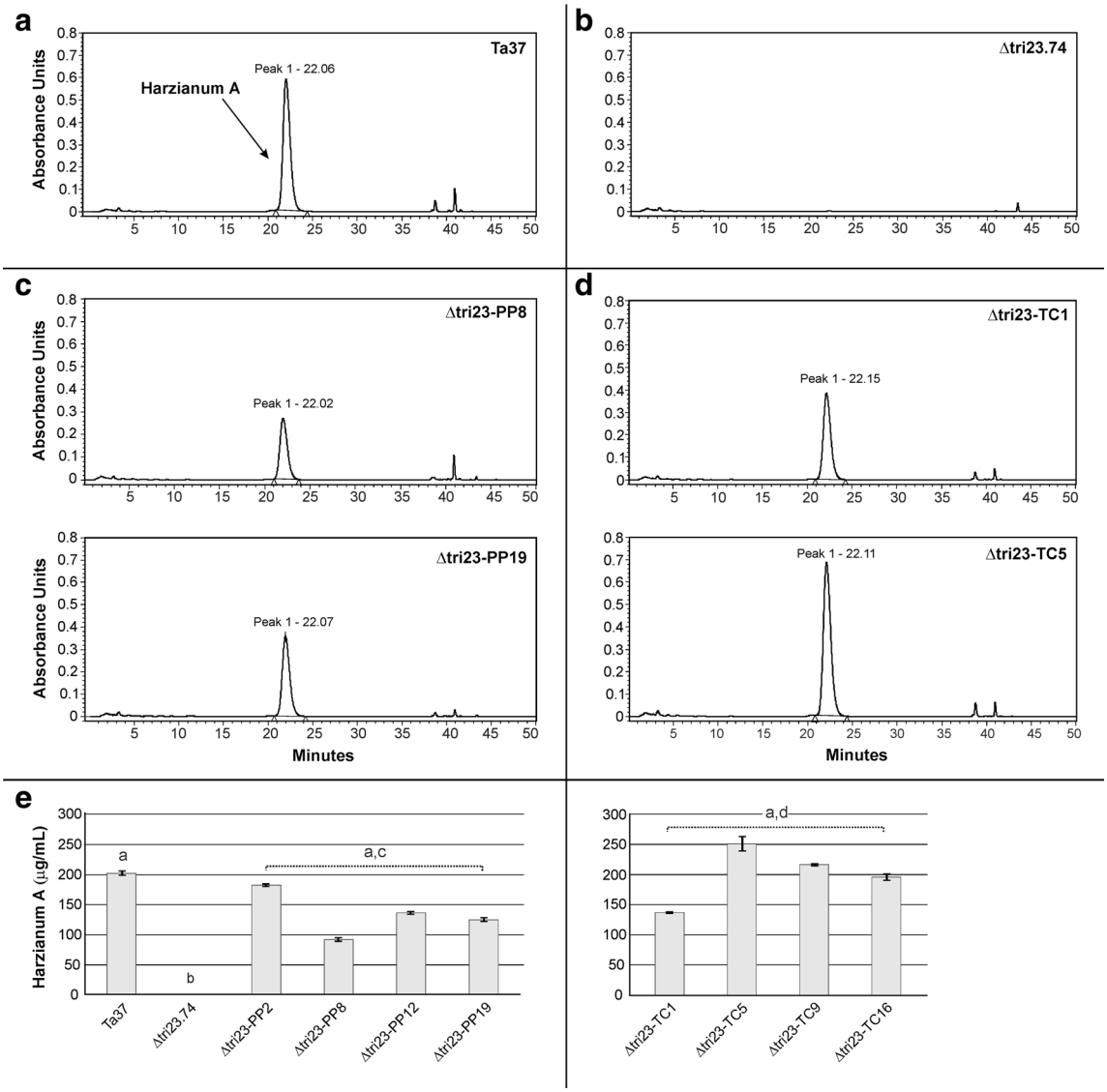

Fig. 6 HPLC chromatograms showing levels of HA produced by **a** wild-type *T. arundinaceum* strain Ta37, **b** *tri23* deletion mutant Δtri23.74, **c** two *tri23*-complemented transformants (strains Δtri23-PP8 and Δtri23-PP19) resulting from transformation of Δtri23.74 with plasmid pPtri23-b1, and **d** two *tri23*-complemented transformants (strains Δtri23-TC1 and Δtri23-TC5) resulting from transformation with plasmid pTCtri23-b1, grown for 48 h in PDB medium. **e** Quantification of HA in the transformants obtained with the plasmids indicated above. Lower case letters above histogram bars indicate statistical significance ($p < 0.05$); bars with different letters are significantly different

Effect of *tri23*-deletion and -complementation on the antifungal activity

Antibiogram assays against *B. cinerea* were performed using 48 h PDB culture broths of *tri23* mutants and the wild-type progenitor strain. The observed antifungal activity was slightly higher with the mutants than with the wild type (Fig. S9a).

Broths from complemented transformants obtained from transformation with pTCtri23-b1 resulted in slightly less growth inhibition than that observed for Ta37 or Δtri23.74 strains (Fig. S9b), even though the complemented mutants had higher levels of *tri23* transcription and HA production. This latter finding indicates that even though HA contributes to the antifungal activity of *T. arundinaceum*, there are other factors (e.g., other secondary metabolites) that also contribute to this activity.

Discussion

Although the genetic bases for structural diversity of *Fusarium* trichothecenes have been largely resolved, much less is known about the genetic bases for structural diversity of trichothecenes produced by other fungi. Nevertheless, recent functional analyses of *tri3*, *tri17*, and *tri18* in *T. arundinaceum* have provided insight into formation of

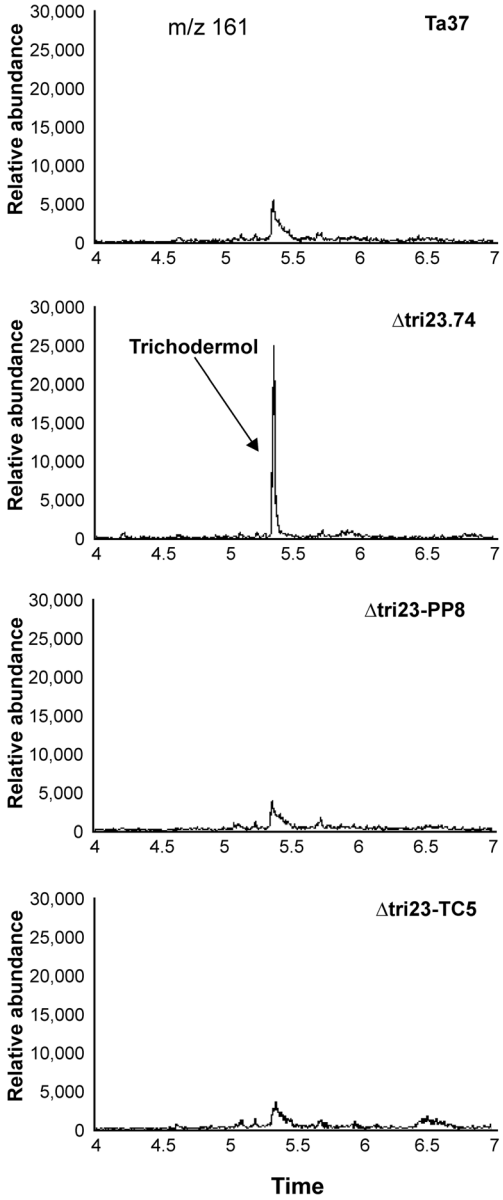

Fig. 7 Gas chromatography-mass spectrometry analysis of extracts of 7-day-old YEPD cultures of wild-type *T. arundinaceum* strain Ta37, *tri23* mutant Δtri23.74, and two *tri23*-complemented mutants derived by transformation of Δtri23.74 with plasmid pPtri23-b1 (Δtri23-PP8) or pPtri23-b1 (Δtri23-TC5). The chromatograms show metabolites with *m/z* (mass-to-charge) 161, which is characteristic of trichodermol

polyketide-derived substituents that occur at C4 of trichothecenes produced by *T. arundinaceum* as well as *Myrothecium*, *Stachybotrys*, and *Trichothecium* species (Lindo et al. 2019a; Proctor et al. 2018). The analyses of these three genes indicate that in *T. arundinaceum* the polyketide synthase TRI17 catalyzes synthesis of octa-2,4,6-trienoic acid, and then acyltransferases TRI3 and TRI18 act in a two-step process that results in esterification of the structurally modified polyketide (i.e., octa-2,4,6-trienedioic acid) to the oxygen atom at C4 of trichodermol. However, information on genes required for structural modifications of the polyketide have been lacking. Thus, in the current study, we identified a CYP gene, *tri23*, and provided evidence that it is required for a modification(s) of octa-2,4,6-trienoic acid.

tri23 was first identified as a potential *tri* gene from among the 91 *T. arundinaceum* CYP genes by its expression, which was affected by *tri6* in a manner similar to previously identified *tri* genes, and by its location next to *tri17* and *tri18*. Because *tri17* and *tri18* are directly involved in formation and esterification of the octa-2,4,6-trienedioyl substituent of HA, the location of *tri23* next to them suggested that it too could be involved in formation of the substituent. Results of deletion and complementation experiments confirmed that *tri23* is required for production of HA but not for trichodermol. This finding was consistent with results from previous studies indicating all enzymes necessary for synthesis of trichodermol from FPP are encoded by *tri5*, *tri4*, and *tri11* (Cardoza et al. 2011; Malmierca et al. 2012, 2013; Proctor et al. 2018; Lindo et al. 2018, 2019b). Further, because the polyketide synthase TRI17 is required for synthesis of the polyketide octa-2,4,6-trienoic acid (Proctor et al. 2018), and because the acyltransferases TRI3 and TRI18 are likely the only genes required for esterification of octa-2,4,6-trienedioic acid to trichodermol (Lindo et al. 2019a), it follows that *tri23* could be involved in conversion of the polyketide to octa-2,4,6-trienedioyl-CoA. This conclusion was further supported by results of cross-culture feeding studies, which demonstrated that during trichothecene biosynthesis TRI23 functions after TRI17.

The mechanism by which octa-2,4,6-trienoic acid in the culture broth of the Δ*tri23* mutant is taken up by cells of the Δ*tri17* mutant is not known. There is evidence that TRI12 and organelles have critical roles in trichothecene export (Kistler and Broz 2015). However, the mechanisms by which trichothecene intermediates are released from fungal cells into the medium are not known, and free diffusion, transmembrane transport, and endocytosis/pinocytosis are all possibilities, as it has been described for the transport of several trichothecene products by mammalian cells (Xiaoming et al. 2017).

Although our results indicate that TRI23 is involved in the conversion of the polyketide octa-2,4,6-trienoic acid to octa-2,4,6-trienedioic acid, the exact function of the enzyme in this conversion process remains to be determined. In order for the conversion to occur, the 8-methyl group of octa-2,4,6-trienoic acid has to be oxidized to form a carboxyl group, a process that should require hydroxylation, alcohol dehydrogenation, and aldehyde dehydrogenation activities. Some CYPs catalyze a single hydroxylation reaction, whereas others catalyze multiple reactions (Urlacher and Girhard 2012). Thus, one possibility is that TRI23 catalyzes hydroxylation of octa-2,4,6-trienoic acid to form the 8-hydroxy derivative of the polyketide (i.e., 8-hydroxy-octa-2,4,6-trienoic acid). However, there are examples of *Arabidopsis*, *Pinus*, and *Fusarium* CYPs that have all three activities necessary to

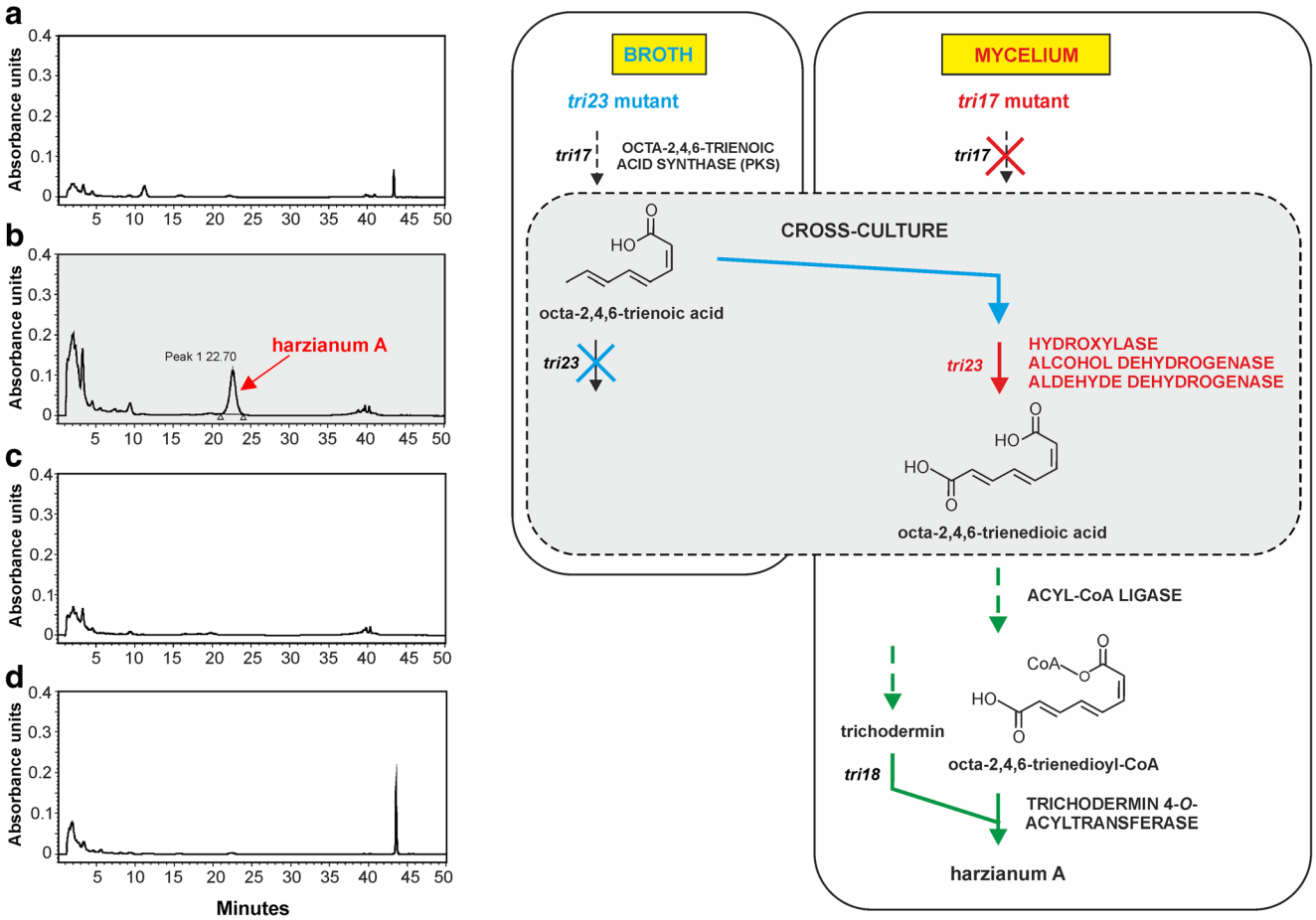

Fig. 8 Results of cross-culture feeding experiments with the *tri17* and *tri123* mutants in which a mutant strain (i.e., *tri23* or *tri17* mutant) was grown in a PDB medium containing extracts of the other mutant. A diagram of the cross-culture feeding protocol is presented in Fig. S8. The left panel shows chromatograms from HPLC analysis of HA in the following treatments: **a** *tri23* mutant grown in the presence of extract of the *tri23* mutant (control); **b** *tri17* mutant grown in presence of extract from the *tri23* mutant; **c** *tri17* mutant grown in the presence of extract of *tri17* mutant (control); **d** *tri23* mutant grown in the presence of extract of *tri17* mutant. HA eluted at approximately 22 min and is indicated with a red arrow in **b**. The right panel illustrates our hypothesis to explain the results of the cross-culture feeding experiments. According to the hypothesis, the *tri23* mutant produces the polyketide octa-2,4,6-trienoic acid but the *tri17* mutant does not. Further, the *tri17* mutant can transform the octa-2,4,6-trienoic acid, which is present in extract from the *tri23* mutant, to octa-2,4,6-trienedioyl-CoA, and in turn use the CoA-activated metabolite to synthesize HA. Blue and red arrows indicate biosynthetic steps that can occur only in the *tri23* (blue) or *tri17* (red) mutant. Green arrows indicate biosynthetic steps that can occur in both mutants

oxidize a methyl group to a carboxyl group (Helliwell et al. 1999; Ro et al. 2005; Tudzynski 2005). Given these precedents, it is possible that TRI23 has all the enzymatic activities necessary for conversion of octa-2,4,6-trienoic acid to octa-2,4,6-trienedioic acid. This hypothesis is consistent with the absence of putative alcohol and aldehyde dehydrogenase genes at the *tri17-tri23-tri18* locus and other known *tri* loci in *T. arundinaceum*. One approach that could be used to elucidate the exact function(s) of TRI23 would be to feed octa-2,4,6-trienoic acid and its 8-hydroxy and 8-carbonyl derivatives to a *T. arundinaceum tri23* mutant to determine which, if any, of the compounds the mutant can convert to octa-2,4,6-trienedioic acid. Similar feeding experiments could also be done with *Saccharomyces cerivisiae* or *Pichia pastoris* strains in which *tri23* is heterologously expressed. However, such experiments will require synthesis of the 8-hydroxy and 8-carbonyl derivatives of octa-2,4,6-trienoic acid as well as development of chromatographic methods that can detect these metabolites and octa-2,4,6-trienedioic acid, tools that are beyond the scope of the current study.

The presence of *tri23* in all HA-producing species of *Trichoderma* examined is consistent with the proposed role of the gene in modification of octa-2,4,6-trienoic acid. *tri23* should not be involved in trichodermin biosynthesis, because the structure of this trichothecene analog does not include an octa-2,4,6-trienedioyl substituent. However, it is not clear why trichodermin-producing species have retained genes that are not required for trichodermin biosynthesis. Nevertheless, the presence of *tri17* and *tri18* in both HA- and trichodermin-producing species suggests

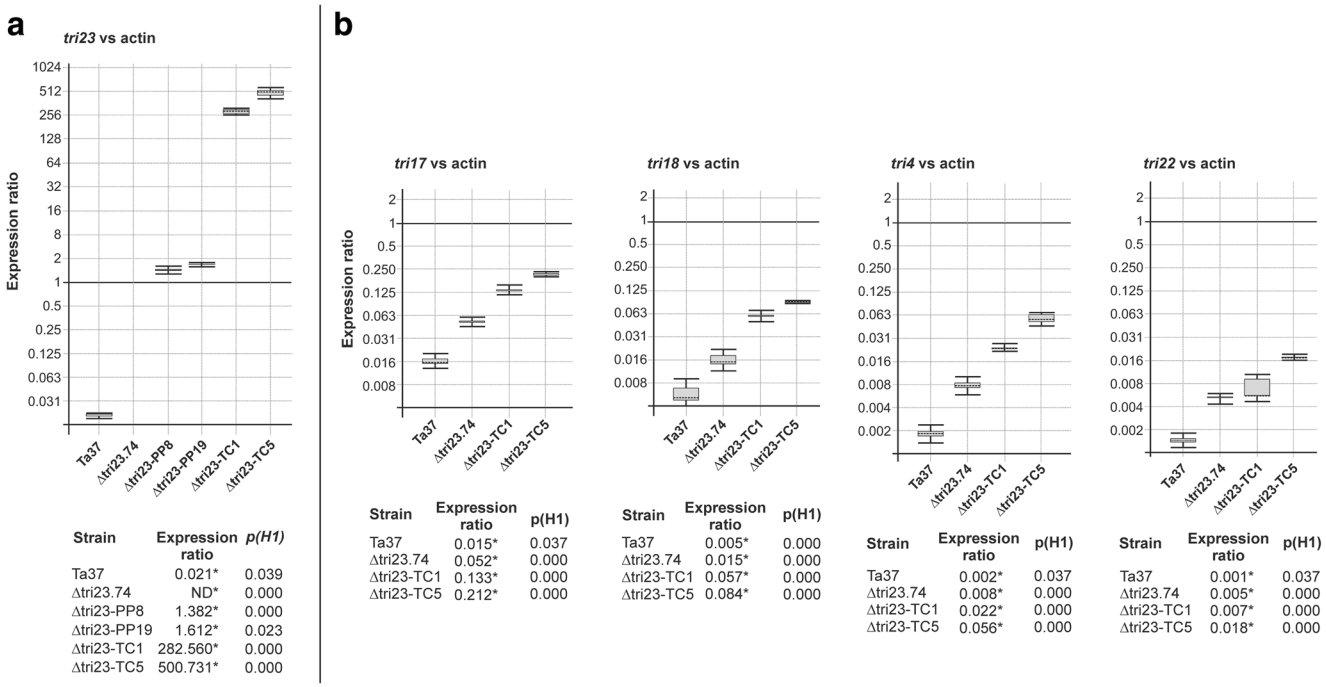

Fig. 9 **a** Quantitative PCR analysis of *tri23* transcription level in wild-type (Ta37), *tri23* mutant (Δtri23.74) and *tri23*-complementation (Δtri23-PP8, Δtri23-PP19, Δtri23-TC1, and Δtri23-TC5) strains of *T. arundinaceum*. **b** Quantitative PCR analysis of transcription of *tri17*, *tri18*, *tri4*, and *tri22* in wild-type (Ta37) and *tri23* mutant (Δtri23.74), and two *tri23*-complementation (Δtri23-TC1 and Δtri23-TC5) strains of *T. arundinaceum*. Transcription levels are ratios calculated relative to the level of transcription of the actin gene. Statistically significant values ($p(H1) < 0.05$) are indicated with an asterisk at the right of the figure. ND, not detected

that HA production constitutes an ancestral state of trichothecene production in *Trichoderma*, whereas trichodermin production constitutes a more derived state.

As noted above, *Myrothecium* and *Stachybotrys* trichothecenes have a polyketide-derived substituent at C4 (Tamm and Breitenstein 1980). The structures of some of the substituents indicate that they are derived from octa-2,4,6-trienoic acid. Like *T. arundinaceum*, trichothecene-producing species of *Myrothecium* and *Stachybotrys* have an ortholog of the polyketide synthase gene *tri17* (Proctor et al. 2018; Semeiks et al. 2014). In addition, the *Myrothecium roridum tri17* ortholog can complement a *tri17* deletion mutant of *T. arundinaceum* (Proctor et al. 2018). These findings indicate that orthologs of the same enzyme (i.e., TRI17) catalyze synthesis of octa-2,4,6-trienoic acid in *Trichoderma*, *Myrothecium* and *Stachybotrys* species. However, the absence of *tri23* in the *Myrothecium* and *Stachybotrys* species indicates that modification of octa-2,4,6-trienoic acid in these fungi involves a gene other than *tri23*.

The 91 predicted CYP genes in the genome sequence of *T. arundinaceum* strain Ta37 is similar to the numbers of CYP genes reported in other *Trichoderma* species. For example, the *T. longibrachiatum* and *T. virens* genomes are predicted to have 68 and 122 CYP genes, respectively (Chadha et al. 2018). The relatively high number of CYP genes in these and other fungi likely reflects their potential to synthesize multiple families of metabolites. Even though CYPs are a common class of secondary metabolite (SM) biosynthetic genes, only 28 out of the 91 *T. arundinaceum* CYP genes (31%) occur in SM gene clusters that were predicted by the program antiSMASH (Lindo et al. 2018).

The finding that 19 *T. arundinaceum* CYPs are members of CYP families that have not been previously reported in other *Trichoderma* species (Chadha et al. 2018) indicates that *T. arundinaceum* biosynthetic potential could differ substantially from other *Trichoderma* species whose CYP gene content has been examined. However, only 9 of this subset of *T. arundinaceum* CYP genes occur in the SM biosynthetic gene clusters predicted by antiSMASH (Table S2). The role of the CYP genes that do not occur in SM clusters could be (i) SM biosynthesis even though they are not located in an obvious cluster, as is the case for some *tri* genes (Proctor et al. 2018); (ii) biosynthesis of primary metabolites such as sterols and aromatic compounds; (iii) catabolic processes such as degradation of xenobiotics (Bernhardt 2006); and/or (iv) metabolism of metabolites that affect interactions with other organisms (Fan et al. 2013).

The increases in production of aspinolides by *tri23* mutants are similar to previously reported increases in aspinolide production in other HA-nonproducing mutants of *T. arundinaceum* (Lindo et al. 2018, 2019b; Malmierca et al. 2015; Susan P. McCormick, unpublished data).

When the various mutants are considered together, it is apparent that the increases occur in mutants in which trichothecene biosynthesis is blocked before formation of EPT, as is the case for *tri5* and *tri6* mutants, as well as in mutants in which the formation of trichothecenes is redirected from HA to trichodermol, as is the case for *tri3*, *tri17*, *tri18*, and *tri23* mutants. The cause(s) of the increased aspinolide production is not clear but has been attributed to changes in levels of acetyl-CoA that likely occur when formation of EPT and/or the octa-2,4,6-trienedioyl substituent is interrupted (Lindo et al. 2018, 2019b). For example, the blocking of EPT formation likely results in accumulation of its precursor FPP, which could in turn result in a buildup of its precursor acetyl-CoA. Such changes could result in rechanneling of acetyl-CoA into polyketide biosynthesis. It is not known whether production of other polyketides is also affected by loss of HA production. Thus, identification of other polyketides produced by *T. arundinaceum* as well as the genes required for their biosynthesis should provide tools that can be used to elucidate the mechanism by which production of aspinolides and perhaps other SMs increases in HA-nonproducing mutants of *T. arundinaceum*.

tri23-deletion resulted in an upregulation of *tri17*, *tri18*, *tri4*, and *tri22* expression compared with the wild-type strain. Furthermore, expression of all *tri* genes analyzed (including *tri23*) was higher in *tri23*-complementation strains compared to the *tri23* mutant. However, even though the transcription levels of these genes were significantly higher in the *tri23*-overexpression strains (Δtri23-TC1 and Δtri23-TC5) than in the wild type, these increases in gene expression did not coincide with consistently higher levels of HA production (see Fig. 6, Fig. 9). This indicates that expression of *tri4*, *tri17*, *tri18*, *tri22*, and *tri23* is not a bottleneck in HA biosynthesis.

In summary, the current study identified *tri23* from among 91 CYP genes in *T. arundinaceum*. The study also provided multiple lines of evidence that the *tri23*-encoded CYP is required for modification of the polyketide octa-2,4,6-trienoic acid during biosynthesis of HA in *T. arundinaceum*, and most likely other HA-producing species of *Trichoderma*. Further, differences in the distribution of *tri23* and the polyketide synthase gene *tri17* among species of trichothecene-producing fungi from multiple genera suggest a common evolutionary origin for synthesis of octa-2,4,6-trienoic acid but different evolutionary origins for subsequent modifications of this polyketide. Thus, the results of the current study provide novel insights into biosynthesis of trichothecenes as well as other fungal secondary metabolites.

Acknowledgements We thank Crystal Probyn, José Alvarez, Jennifer Teresi, Amy McGovern, and Christine Hodges for technical assistance.

Data Availability Statement Sequences of the genomic regions containing *tri18-tri17* and *tri23* when present, from *Trichoderma protrudens*, *T. turrialbense*, *T. albolutescens*, and *Hypocrea rodmanii*, have been submitted to the GenBank database of the National Center for Biotechnology Information. The accession numbers for these sequences are as follows: MN136191 *Hypocrea rodmanii*, MN136192 *T. albolutescens*, MN136193 *T. protrudens*, and MN136194 *T. turrialbense*.

Genome sequences of *T. arundinaceum* and *T. brevicompactum* are available (Proctor et al. 2018).

Funding This work was supported by the Spanish Ministry of Science, Innovation and Universities (MICINN-RTI2018-099600-B-100 to S.G.). Funding was also provided by the USDA-ARS National Program for Food Safety (NP108). L. Lindo was granted a fellowship by the University of León (Spain).

Compliance with ethical standards

Conflict of interest The authors declare that they have no conflict of interest.

Ethical approval This article does not contain any studies with human or animals performed by any of the authors.

Disclaimer Mention of trade names or commercial products in this article is solely for the purpose of providing specific information and does not imply recommendation or endorsement by the US Department of Agriculture. USDA is an equal opportunity provider and employer.

References

Alexander NJ, McCormick SP, Hohn TM (1999) TRI12, a trichothecene efflux pump from *Fusarium sporotrichioides*: gene isolation and expression in yeast. Mol Gen Genet 261:977–984

Bernhardt R (2006) Cytochromes P450 as versatile biocatalysts. J Biotechnol 124:128–145. https://doi.org/10.1016/j.jbiotec.2006.01.026

Cardoza RE, Vizcaino JA, Hermosa MR, Monte E, Gutiérrez S (2006) A comparison of the phenotypic and genetic stability of recombinant *Trichoderma* spp. generated by protoplast- and *Agrobacterium*-mediated transformation. J Microbiol 44:383–395

Cardoza RE, Malmierca MG, Hermosa MR, Alexander NJ, McCormick SP, Proctor RH, Tijerino AM, Rumbero A, Monte E, Gutiérrez S (2011) Identification of loci and functional characterization of trichothecene biosynthesis genes in filamentous fungi of the genus *Trichoderma*. Appl Environ Microbiol 77:4867–4877. https://doi.org/10.1128/AEM.00595-11

Cardoza RE, McCormick SP, Malmierca MG, Olivera ER, Alexander NJ, Monte E, Gutiérrez S (2015) Effects of trichothecene production on the plant defense response and fungal physiology: overexpression of the *Trichoderma arundinaceum tri4* gene in *T. harzianum*. Appl Environ Microbiol 81:6355–6366. https://doi.org/10.1128/AEM.01626-15

Chadha S, Mehetre ST, Bansl R, Kuo A, Aerts A, Grigoriev IV, Druzhinina IS, Mukherjee PK (2018) Genome-wide analysis of cytochrome P450s of *Trichoderma* spp.: annotation and evolutionary relationships. Fungal Biol Biotechnol 5:12. https://doi.org/10.1186/s40694-018-0056-3

Chen W, Lee MK, Jefcoate C, Kim SC, Chen F, Yu JH (2014) Fungal cytochrome p450 monooxygenases: their distribution, structure, functions, family expansion, and evolutionary origin. Genome Biol Evol 6:1620–1634. https://doi.org/10.1093/gbe/evu132

Crooks GE, Hon G, Chandonia J-M, Brenner SE (2004) WebLogo: a sequence logo generator. Genome Res 14:1188–1190. https://doi.org/10.1101/gr.849004

Fan J, Urban M, Parker JE, Brewer HC, Kelly SL, Hammond-Kosack KE, Fraaije BA, Liu X, Cools HJ (2013) Characterization of the sterol 14α-demethylases of *Fusarium graminearum* identifies a novel genus-specific CYP51 function. New Phytol 198:821–835. https://doi.org/10.1111/nph.12193

Harman GE, Howell CR, Viterbo A, Chet I, Lorito M (2004) *Trichoderma* species–opportunistic, avirulent plant symbionts. Nat Rev Microbiol 2:43–56. https://doi.org/10.1038/nrmicro797

Helliwell CA, Poole A, Peacock J, Dennis ES (1999) *Arabidopsis ent*-kaurene oxidase catalyzes three steps of gibberellin biosynthesis. Plant Physiol 119:507–510

Hermosa R, Viterbo A, Chet I, Monte E (2012) Plant-beneficial effects of *Trichoderma* and of its genes. Microbiology (Reading, Engl) 158: 17–25. https://doi.org/10.1099/mic.0.052274-0

Hillis DM, Bull JJ (1993) An empirical test of bootstrapping as a method for assessing confidence in phylogenetic analysis. Syst Biol 42:182–192. https://doi.org/10.1093/sysbio/42.2.182

Hofmann K, Stoffel W (1993) TMbase - a database of membrane spanning proteins segments. Biol Chem Hoppe Seyler 374:166

Hohn TM, Krishna R, Proctor RH (1999) Characterization of a transcriptional activator controlling trichothecene toxin biosynthesis. Fungal Genet Biol 26:224–235. https://doi.org/10.1006/fgbi.1999.1122

Käll L, Krogh A, Sonnhammer ELL (2004) A combined transmembrane topology and signal peptide prediction method. J Mol Biol 338: 1027–1036. https://doi.org/10.1016/j.jmb.2004.03.016

Katoh K, Miswa K, Kuma K-I, Miyata T (2002) MAFFT: a novel method for rapid multiple sequence alignment based on fast Fourier transform. Nucleic Acids Res 30:3059–3066

Kikuchi H, Miyagawa Y, Sahashi Y, Inatomi S, Haganuma A, Nakahata N, Oshima Y (2004) Novel spirocyclic trichothecanes, spirotenuipesine A and B, isolated from entomopathogenic fungus, *Paecilomyces tenuipes*. J Org Chem 69:352–356. https://doi.org/10.1021/jo035137x

Kistler HC, Broz K (2015) Cellular compartmentalization of secondary metabolism. Front Microbiol 6:68. https://doi.org/10.3389/fmicb.2015.00068

Krogh A, Larsson B, von Heijne G, Sonnhammer EL (2001) Predicting transmembrane protein topology with a hidden Markov model: application to complete genomes. J Mol Biol 305:567–580. https://doi.org/10.1006/jmbi.2000.4315

Kumar S, Stecher G, Tamura K (2016) MEGA7: molecular evolutionary genetics analysis version 7.0 for bigger datasets. Mol Biol Evol 33: 1870–1874. https://doi.org/10.1093/molbev/msw054

Lamb DC, Skaug T, Song H-L, Jackson CJ, Podust LM, Waterman MR, Kell DB, Kelly DE, Kelly SL (2002) The cytochrome P450 complement (CYPome) of *Streptomyces coelicolor* A3(2). J Biol Chem 277:24000–24005. https://doi.org/10.1074/jbc.M111109200

Lee HB, Kim Y, Jin HZ, Lee JJ, Kim C-J, Park JY, Jung HS (2005) A new *Hypocrea* strain producing harzianum A cytotoxic to tumour cell lines. Lett Appl Microbiol 40:497–503. https://doi.org/10.1111/j.1472-765X.2005.01719.x

Lindo L, McCormick SP, Cardoza RE, Brown DW, Kim H-S, Alexander NJ, Proctor RH, Gutiérrez S (2018) Effect of deletion of a trichothecene toxin regulatory gene on the secondary metabolism transcriptome of the saprotrophic fungus *Trichoderma arundinaceum*. Fungal Genet Biol 119:29–46. https://doi.org/10.1016/j.fgb.2018.08.002

Lindo L, McCormick SP, Cardoza RE, Busman M, Alexander NJ, Proctor RH, Gutiérrez S (2019a) Requirement of two acyltransferases for 4-O-acylation during biosynthesis of harzianum A, an antifungal trichothecene produced by *Trichoderma arundinaceum*. J Agric Food Chem 67:723–734. https://doi.org/10.1021/acs.jafc.8b05564

Lindo L, McCormick SP, Cardoza RE, Kim H-S, Brown DW, Alexander NJ, Proctor RH, Gutiérrez S (2019b) Role of *Trichoderma arundinaceum tri10* in regulation of terpene biosynthetic genes and in control of metabolic flux. Fungal Genet Biol 122:31–46. https://doi.org/10.1016/j.fgb.2018.11.001

Malmierca MG, Cardoza RE, Alexander NJ, McCormick SP, Hermosa R, Monte E, Gutiérrez S (2012) Involvement of *Trichoderma* trichothecenes in the biocontrol activity and induction of plant defense-related genes. Appl Environ Microbiol 78:4856–4868. https://doi.org/10.1128/AEM.00385-12

Malmierca MG, Cardoza RE, Alexander NJ, McCormick SP, Collado IG, Hermosa R, Monte E, Gutiérrez S (2013) Relevance of trichothecenes in fungal physiology: disruption of *tri5* in *Trichoderma arundinaceum*. Fungal Genet Biol 53:22–33. https://doi.org/10.1016/j.fgb.2013.02.001

Malmierca MG, Barua J, McCormick SP, Izquierdo-Bueno I, Cardoza RE, Alexander NJ, Hermosa R, Collado IG, Monte E, Gutiérrez S (2015) Novel aspinolide production by *Trichoderma arundinaceum* with a potential role in *Botrytis cinerea* antagonistic activity and plant defence priming. Environ Microbiol 17:1103–1118. https://doi.org/10.1111/1462-2920.12514

McCormick SP, Stanley AM, Stover NA, Alexander NJ (2011) Trichothecenes: from simple to complex mycotoxins. Toxins 3: 802–814. https://doi.org/10.3390/toxins3070802

Nakamura T, Yamada KD, Tomii K, Katoh K (2018) Parallelization of MAFFT for large-scale multiple sequence alignments. Bioinformatics 34:2490–2492. https://doi.org/10.1093/bioinformatics/bty121

Nasmith CG, Walkowiak S, Wang L, Leung WWY, Gong Y, Johnston A, Harris LJ, Guttman DS, Subramaniam R (2011) Tri6 is a global transcription regulator in the phytopathogen *Fusarium graminearum*. PLoS Pathog 7:e1002266. https://doi.org/10.1371/journal.ppat.1002266

Nelson DR (1999) Cytochrome P450 and the individuality of species. Arch Biochem Biophys 369:1–10. https://doi.org/10.1006/abbi.1999.1352

Nelson DR (2018) Cytochrome P450 diversity in the tree of life. Biochim Biophys Acta, Proteins Proteomics 1866:141–154. https://doi.org/10.1016/j.bbapap.2017.05.003

Nguyen L-T, Schmidt HA, von Haeseler A, Minh BQ (2014) IQ-TREE: A fast and effective stochastic algorithm for estimating maximum-likelihood phylogenies. Mol Biol Evol 32:268–274. https://doi.org/10.1093/molbev/msu300

Petersen TN, Brunak S, von Heijne G, Nielsen H (2011) SignalP 4.0: discriminating signal peptides from transmembrane regions. Nat Methods 8:785–786. https://doi.org/10.1038/nmeth.1701

Pfaffl MW, Horgan GW, Dempfle L (2002) Relative expression software tool (REST) for group-wise comparison and statistical analysis of relative expression results in real-time PCR. Nucleic Acids Res 30: e36

Pitt JI, Lange L, Lacey AE, Vuong D, Midgley DJ, Greenfield P, Bradbury MI, Lacey E, Busk PK, Pilgaard B, Chooi Y-H, Piggott AM (2017) *Aspergillus hancockii* sp. nov., a biosynthetically talented fungus endemic to southeastern Australian soils. PLoS ONE 12: e0170254. https://doi.org/10.1371/journal.pone.0170254

Poulos T, Johnson E (2005) Structures of cytochrome P450 enzymes. In: Cytochrome P450. Structure, mechanism and biochemistry. Kluwer Academic, New York, pp 88–114

Proctor RH, Desjardins AE, Plattner RD, Hohn TM (1999) A polyketide synthase gene required for biosynthesis of fumonisin mycotoxins in *Gibberella fujikuroi* mating population A. Fungal Genet Biol 27: 100–112. https://doi.org/10.1006/fgbi.1999.1141

Proctor RH, McCormick SP, Kim H-S, Cardoza RE, Stanley AM, Lindo L, Kelly A, Brown DW, Lee T, Vaughan MM, Alexander NJ, Busman M, Gutiérrez S (2018) Evolution of structural diversity of trichothecenes, a family of toxins produced by plant pathogenic and

entomopathogenic fungi. PLoS Pathog 14:e1006946. https://doi.org/10.1371/journal.ppat.1006946

Punt PJ, Oliver RP, Dingemanse MA, Pouwels PH, van den Hondel CA (1987) Transformation of *Aspergillus* based on the hygromycin B resistance marker from *Escherichia coli*. Gene 56:117–124

Quidde T, Osbourn AE, Tudzynski P (1998) Detoxification of α-tomatine by *Botrytis cinerea*. Physiol Mol Plant Pathol 52:151–165

Ro DK, Arimura GI, Lau SYW, Piers E, Bohlmann J (2005) Loblolly pine abietadienol/abietadienal oxidase *PtAO* (CYP702B1) is a multifunctional, multisubstrate cytochrome P450 monooxygenase. Proc Natl Acad Sci U S A 102:8060–8065. https://doi.org/10.1073/pnas.0500825102

Rubio MB, Hermosa R, Vicente R, Gómez-Acosta FA, Morcuende R, Monte E, Bettiol W (2017) The combination of *Trichoderma harzianum* and chemical fertilization leads to the deregulation of phytohormone networking, preventing the adaptive responses of tomato plants to salt stress. Front Plant Sci 8:294. https://doi.org/10.3389/fpls.2017.00294

Ryu SM, Lee HM, Song EG, Seo YH, Lee J, Guo Y, Kim BS, Kim J-J, Hong JS, Ryu KH, Lee D (2017) Antiviral activities of trichothecenes isolated from *Trichoderma albolutescens* against pepper mottle virus. J Agric Food Chem 65:4273–4279. https://doi.org/10.1021/acs.jafc.7b01028

Saitou N, Nei M (1987) The neighbor-joining method: a new method for reconstructing phylogenetic trees. Mol Biol Evol 4:406–425. https://doi.org/10.1093/oxfordjournals.molbev.a040454

Schneider TD, Stephens RM (1990) Sequence logos: a new way to display consensus sequences. Nucleic Acids Res 19:6097–6100

Semeiks J, Borek D, Otwinowski Z, Grishin NV (2014) Comparative genome sequencing reveals chemotype-specific gene clusters in the toxigenic black mold *Stachybotrys*. BMC Genomics 15:590. https://doi.org/10.1186/1471-2164-15-590

Shoresh M, Harman GE, Mastouri F (2010) Induced systemic resistance and plant responses to fungal biocontrol agents. Annu Rev Phytopathol 48:21–43. https://doi.org/10.1146/annurev-phyto-073009-114450

Sievers F, Higgins DG (2014) Clustal Omega, accurate alignment of very large numbers of sequences. Methods Mol Biol 1079:105–116. https://doi.org/10.1007/978-1-62703-646-7_6

Sievers F, Wilm A, Dineen D, Gibson TJ, Karplus K, Li W, Lopez R, McWilliam H, Remmert M, Söding J, Thompson JD, Higgins DG (2011) Fast, scalable generation of high-quality protein multiple sequence alignments using Clustal Omega. Mol Syst Biol 7:539. https://doi.org/10.1038/msb.2011.75

Tamm C, Breitenstein W (1980) The biosynthesis of trichothecene mycotoxins. In: The biosynthesis of mycotoxins: a study in secondary metabolism. Elsevier, New York, pp 69–101

Tudzynski B (2005) Gibberellin biosynthesis in fungi: genes, enzymes, evolution, and impact on biotechnology. Appl Microbiol Biotechnol 66:597–611. https://doi.org/10.1007/s00253-004-1805-1

Urlacher VB, Girhard M (2012) Cytochrome P450 monooxygenases: an update on perspectives for synthetic application. Trends Biotechnol 30:26–36. https://doi.org/10.1016/j.tibtech.2011.06.012

Werck-Reichhart D, Feyereisen R (2000) Cytochromes P450: a success story. Genome Biol 1:3003.1–3003.9. https://doi.org/10.1186/gb-2000-1-6-reviews3003

Xiaoming L, Mu P, Wen J, Deng Y (2017) Carrier-mediated and energy-dependent uptake and efflux of deoxynivalenol in mammalian cells. Sci Rep 5:5889. https://doi.org/10.1038/s41598-017-06199-8